Vol 17 No 12, December 2008
1674-1056/2008/17(12)/4554-08

Chinese Physics B

© 2008 Chin. Phys. Soc.
and IOP Publishing Ltd

The effect of surface roughness on rarefied gas flows by lattice Boltzmann method*

Liu Chao-Feng(刘超峰) and Ni Yu-Shan(倪玉山)†

Department of Mechanics and Engineering Science, Fudan University, Shanghai 200433, *China*

(Received 1 February 2008; revised manuscript received 30 June 2008)

This paper studies the roughness effect combining with effects of rarefaction and compressibility by a lattice Boltzmann model for rarefied gas flows at high Knudsen numbers. By discussing the effect of the tangential momentum accommodation coefficient on the rough boundary condition, the lattice Boltzmann simulations of nitrogen and helium flows are performed in a two-dimensional microchannel with rough boundaries. The surface roughness effects in the microchannel on the velocity field, the mass flow rate and the friction coefficient are studied and analysed. Numerical results for the two gases in micro scale show different characteristics from macroscopic flows and demonstrate the feasibility of the lattice Boltzmann model in rarefied gas dynamics.

Keywords: surface roughness, lattice Boltzmann method, rarefied gas flows, velocity slip
PACC: 4760, 4745G, 4710

1. Introduction

Surface roughness is identified as an important factor in liquid or gas flows. The well-known Moody diagram.[1] have successfully served countless engineers over the last many decades. In the Moody diagram, the relationship between the Darcy friction factor and the Reynolds number over various values of 5% or less[2] of the relative roughness (the ratio of the roughness height to the channel height) in a macro fluid flow system is plotted. However, the value of the relative roughness is taken frequently beyond 5% when the effect of surface roughness is enhanced in a micro fluid flow system.[2] As the development of Micro-Electro-Mechanical Systems (MEMS), more and more industrial problems require a deep understanding of the effects of surface roughness on the micro flow systems.

It is known that the micro gas flows (generally the rarefied gas flows) can be divided into four areas by the Knudsen number: (a) $Kn < 0.001$, the continuum region; (b) $0.001 < Kn < 0.1$, the slip flow region; (c) $0.1 < Kn < 10$, the transition region; (d) $Kn > 10$, the free molecule region. The finite Knudsen numbers in (b) and (c) are commonly used in MEMS. In the above two regions, slip boundary condition must be applied or the kinetic Boltzmann equation needs to be solved, while the Navier–Stokes equation with the non-slip boundary condition is not directly applied. Thus, molecular-based models including molecular dynamics simulations, Boltzmann equation and direct simulations Monte Carlo are used in modelling the flows at high Knudsen numbers.[3] Recently, Turner *et al*[4] measured the friction coefficient of slip flows of air and helium in microchannels and observed that the surface roughness might cause a larger friction than the theoretical prediction. Mala and Li.[5] experimentally investigated water flow through microtubes with diameters ranging from 50 to 254μm. Shen *et al*[6] did experiments to investigate liquid flow and heat transfer in 26 rectangular microchannels of 300μm width and 800μm depth. By computational simulations, Sugiyama *et al*[7] investigated the free-molecule and near-free-molecule flow conductance through microchannels using Monte-Carlo method. Sun and Faghri[8] performed a direct Monte-Carlo simulation to find the increase of the friction coefficient with increasing roughness height and decreasing distance between the roughness modules. Ding *et al*[9] investigated nitrogen gas flow characteristics through four trapezoidal silicon microchannels with different hydraulic diameters. Cao *et al*[10−12] studied the effect of surface roughness on the boundary conditions and the friction characteristics by molecular dynamic

*Project supported by the National Natural Science Foundation of China and NSAF (Grant No 10576010), and by the Creation Foundation of Fudan University (Grant No 2126003).
†Corresponding author. E-mail: niyushan@fudan.edu.cn

simulation. The above experiments and simulations exemplified the significance of understanding surface roughness effects in microchannels.

The lattice Boltzmann method provides a new effective way to study micro flow systems from the pioneer lattice Boltzmann models for micro flows designed by Nie *et al*[13] and Lim *et al.*[14] However, Shen *et al*[15] pointed out that Nie's model was not feasible for a large negative deviation of pressure distribution when $Kn > 0.1$. Recently, Succi *et al*,[16−19] Ansumali and Karlin.[20,21] and some other authors[14,22−27] developed the method and studied micro flows using lattice Boltzmann method in microchannels with smooth boundaries. The above researches have indicated that the results by lattice Boltzmann method were consistent with the theoretical studies and experiments. Compared with molecular dynamic simulation, direct Monte-Carlo simulation and other related methods, the lattice Boltzmann method gains the advantages of computational efficiency and the flexibility for complex boundary geometries.

Few lattice Boltzmann researchers up to now have concentrated on the micro gas flows in rough boundaries even though the roughness effect becomes more significant in micro scales. Thus, to understand the effect of surface roughness on the micro flow systems, we here design a lattice Boltzmann model which can simulate rarefied gas flows at high Knudsen numbers, deduct the expression of relaxation time as a function of the dynamical viscosity and the density, and discuss the influence of the tangential momentum accommodation coefficient on the slip velocity at the rough boundaries. Finally, we study and analyse the effects of relative roughness on the velocity field, the mass flow rate and the friction coefficient of the micro flows of helium and nitrogen.

2. Theory and deduction

2.1. Lattice Boltzmann model at high Knudsen number

The starting point of the rarefied gas dynamics is the kinetic Boltzmann equation. In the Boltzmann equation, the state of a single gas is described by the distribution function $f(\boldsymbol{x}, t, \boldsymbol{v})$, where $\boldsymbol{x}$ is the spatial coordinates vector, t is the time and $\boldsymbol{v}$ is the velocity of molecules. Defining the distribution function, we get the Boltzmann equation without an external force:

$$\frac{\partial f}{\partial t} + \boldsymbol{v} \cdot \frac{\partial f}{\partial \boldsymbol{x}} = Q(ff_*), \tag{1}$$

where $Q(ff_*)$ is the collision integral and it obeys the conservation equations and the principle of increase of entropy:

$$\int \psi(\boldsymbol{v}) Q(ff_*) \mathrm{d}\boldsymbol{v} = 0,$$

$$\psi(\boldsymbol{v}) = 1, \quad m\boldsymbol{v}, \quad \frac{1}{2} m\boldsymbol{v}^2, \tag{2}$$

$$\int Q(ff_*) \ln f \mathrm{d}\boldsymbol{v} \leq 0. \tag{3}$$

The computational complexity does not allow us to calculate the collision integral directly in the Boltzmann equation; therefore a number of approximate methods of solving the Boltzmann equation were developed. Among these model equations, Bhatnagar, Gross and Krook[28] (BGK) model simplify the collision integral as:

$$Q(ff_*) = -\frac{1}{\tau(\boldsymbol{x}, t)} (f(\boldsymbol{x}, t, \boldsymbol{v}) - f^{\mathrm{eq}}(\boldsymbol{x}, t)), \tag{4}$$

where τ is the relaxation time and f^{eq} is the equilibrium distribution function of local Maxwellian. In Eq.(4), τ and f^{eq} are assumed to be independent of the molecular velocity via the macroscopic quantities: density ρ and velocity $\boldsymbol{u}$. Here we can verify that the BGK model (4) obeys the fundamental laws of Eq.(2) and Eq.(3).

The pioneer applications of the lattice BGK equation for microflows were proposed by Nie *et al*[13] and Lim *et al.*[14] However, Nie's model with a bounce-back boundary condition is argued to be flawed for numerical artificial.[15] Ansumali and Karlin[20,21] designed an improved scheme of isothermal entropy lattice BGK model as follows:

$$f_i(\boldsymbol{x}+\delta\boldsymbol{x}, t+\delta t) - f_i(\boldsymbol{x}, t) = -\frac{\delta t}{\tau + \frac{1}{2}\delta t} \left(f_i - f_i^{\mathrm{eq}}\right), \tag{5}$$

where $\delta\boldsymbol{x}$ and δt are the space step and the time step respectively. The local equilibrium $f_i^{\mathrm{eq}}, i = 0, \ldots, 1.8$ in Eq.(5) is the conditional minimization of the entropy function which is defined in Refs.[20, 21] and the expression for the D2Q9 model is the well-known local equilibrium of Qian:[29]

$$f_i^{\mathrm{eq}} = w_i \rho \left[1 + \frac{3}{c^2}(\boldsymbol{c}_i \cdot \boldsymbol{u}) + \frac{9}{2c^4}(\boldsymbol{c}_i \cdot \boldsymbol{u})^2 - \frac{3}{2c^2} u^2\right], \tag{6}$$

where $\boldsymbol{c}_i$ is the particle velocity and $c = \sqrt{3RT}$ (for the D2Q9 model), R is the gas constant and T is the gas temperature. The weighting coefficients are: $w_0 = 4/9$; $w_i = 1/9$, $i = 1, 2, 3, 4$; $w_i = 1/36$,

$i = 5, 6, 7, 8$. The pressure in the D2Q9 model is given by

$$P = \frac{1}{3}c^2\rho. \tag{7}$$

In Eq.(5), τ is the only undetermined parameter which depends on the properties of the investigated gas. Specifically, it can also be defined as a function of the dynamic viscosity and the pressure in the lattice Boltzmann model:[29]

$$\tau = \frac{\mu}{P}. \tag{8}$$

Equation (8) implies the physical characteristic that the relaxation time is in direct proportion with viscosity and in inverse proportion with pressure. As is known, the Knudsen number is defined as $Kn = \lambda/H$, where H is the characteristic length and λ is the mean free path of the gas flow. Here we take H as the height of the channel. To deduce the relationship between τ and Kn in the lattice Boltzmann model, the alternative expression in terms of the mean free path can be used:[30−32]

$$\tau = \frac{\lambda}{c*}, \tag{9}$$

where $c*$ is a certain microscopic velocity to be determined. It is noted that the choice of $c*$ is rather diverse in the present literatures. The lattice velocity c is widely applied[14,18,19,23] and the mean thermal velocity of gas molecules $\bar{c} = \sqrt{\dfrac{8RT}{\pi}}$[22,33] is also adopted. However, Guo *et al*[30,31] pointed out that the choice of $c*$ should satisfy the 'consistent requirement' as $Kn \to 0$ in the lattice Boltzmann scheme. With the choice of $c* = \sqrt{\dfrac{\pi RT}{2}}$, the Knudsen number as a function of the relaxation time is obtained:[30,31]

$$Kn = \frac{\tau}{H}c* = \frac{\tau}{H}\sqrt{\frac{\pi RT}{2}}. \tag{10}$$

By determining the value of the relaxation time and the Knudsen number of the investigated gas, the lattice Boltzmann model simulating micro rarefied flows has been ascertained completely.

2.2. Discussions for the treatment of rough boundary

To simulate the rarefied gas flows or the gas flows in a microchannel, the following two aspects need to be studied in the lattice Boltzmann model: deciding the relaxation time and choosing a suitable boundary condition. The former indicates the state equation of the investigated gas and the latter describes the gas-wall interaction. Hence the treatment of the boundary conditions is a very important aspect in the lattice Boltzmann method. In the present lattice Boltzmann methods the bounce conditions show great advantages when dealing with flows in complex geometries.[18,34] The bounce-back (bb) rule and the bounce-forward (bf) rule are the two familiar bounce wall boundary conditions as illustrated in Fig.1.[35] The bb collision rule has the approximate physical effect of no-slip boundary, namely the tangential velocity $u = 0$ (macro flow system) and normal velocity $v = 0$ close to the wall. The treatment of bb boundary is simple and direct in the lattice Boltzmann method, namely the incident particles bounce back along the incident direction. The bf collision rule has the approximate physical effect of full slip boundary, namely the tangential velocity $u =$ const and the normal velocity $v = 0$. The treatment of bf boundary in the lattice Boltzmann method is that the incident particles slip forward along the specular direction.

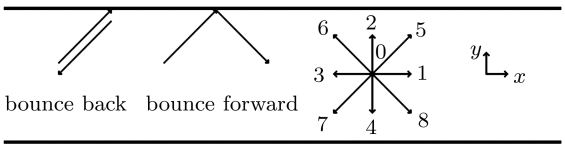


Fig.1. The bounce-back boundary condition and the bounce-forward boundary condition on the wall.

The actual slip boundary in microchannels should comprise partial bb rule and partial bf rule. To capture the physical slip velocity component on the wall, the tangential momentum accommodation coefficient σ is used to measure its integral characteristics. The accommodation coefficient can be defined as the proportion of diffuse reflected particles (the slip-reflection mode).[18,34] On a constant temperature wall, the expression of slip velocity deduced by Maxwell from kinetic theory of rarefied monatomic gases is[36]

$$u_{\text{slip}} - u_{\text{wall}} = \frac{2-\sigma}{\sigma}\lambda\left.\frac{\partial u}{\partial n}\right|_{\text{wall}}. \tag{11}$$

Further, the second order slip boundary condition presented by Hadjiconstantinou[37] for a hard sphere gas in the condition of fully-diffusive reflection is

$$u_{\text{slip}} = 1.1466\lambda\left.\frac{\partial u}{\partial n}\right|_{\text{wall}} + 2\times 0.31\lambda^2\left.\frac{\partial^2 u}{\partial n^2}\right|_{\text{wall}}. \tag{12}$$

Zhang *et al*[22,34] introduced the coefficient $\dfrac{2-\sigma}{\sigma}$ into the first term of Eq.(12), the expression of velocity

profile in the Maxwellian scattering model is obtained as

$$u_{\text{slip}} = -\frac{\mathrm{d}P}{\mathrm{d}x}\frac{H^2}{2\mu}\left(\frac{2-\sigma}{\sigma}\times 1.1466Kn + 2\times 0.31Kn^2\right). \tag{13}$$

Since our aim is to study the effect of surface roughness in micro flow domain, a two-dimensional self-affine fractal boundary should be created at the beginning of the simulation. The independent division method in Ref.[38] is employed to create the surface. Suppose the function for the boundary surface is $y(x)$, the amplitude of the rough surface can be defined as

$$\Lambda^2 = \left\langle [y(x) - \langle y(x)\rangle]^2 \right\rangle = \frac{1}{L}\int_0^L [y(x) - \langle y(x)\rangle]^2\,\mathrm{d}x. \tag{14}$$

Then the relative roughness of the boundary surface is defined as:

$$\Delta = \frac{\Lambda}{H}. \tag{15}$$

Irregular obstacles will appear in the internal nodes of the lattice Boltzmann model when treating the fractal tips with rectangular grid. And the accommodation coefficient is implemented into the irregular wall. As shown in Fig.2, the bounce rule in the lattice Boltzmann model of D2Q9 which is proposed by Succi *et al*[18,34] is given on the bottom wall:

$$\begin{aligned} f_2(x,y,t+\delta t) &= f_4(x,y+\delta y,t),\\ f_5(x,y,t+\delta t) &= \sigma f_7(x+\delta x,y+\delta y,t) + (1-\sigma) f_8(x-\delta x,y+\delta y,t),\\ f_6(x,y,t+\delta t) &= \sigma f_8(x-\delta x,y+\delta y,t) + (1-\sigma) f_7(x+\delta x,y+\delta y,t). \end{aligned} \tag{16}$$

And the bounce rule on the left wall is

$$\begin{aligned} f_1(x,y,t+\delta t) &= f_3(x+\delta x,y,t),\\ f_5(x,y,t+\delta t) &= \sigma f_7(x+\delta x,y+\delta y,t) + (1-\sigma) f_6(x-\delta x,y-\delta y,t),\\ f_8(x,y,t+\delta t) &= \sigma f_6(x-\delta x,y-\delta y,t) + (1-\sigma) f_7(x+\delta x,y+\delta y,t). \end{aligned} \tag{17}$$

Similar procedures can be applied on the top wall and the right wall, respectively.

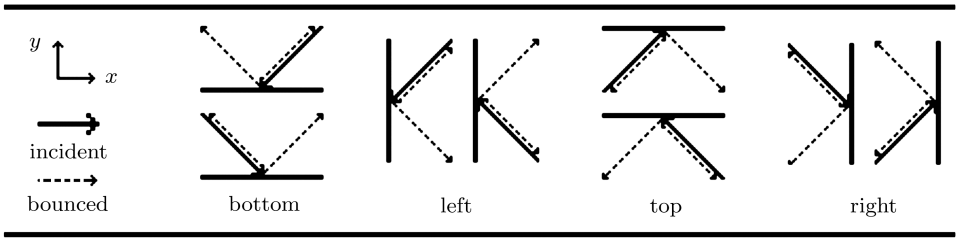


Fig.2. The bounce rules on the irregular wall.

An accurate determination of the value of the accommodation coefficient σ is the most important aspect in a lattice Boltzmann simulation to describe the wall interaction with gas particles. Figure 3 shows the velocity profiles at the position of $x = L/2$ at various values of σ. It is noted that the limit of $\sigma = 0$ in Fig.3 corresponds to the case of bf boundary and the limit of $\sigma = 1$ corresponds to the case of bb boundary in the lattice Boltzmann simulation. We can see in Fig.3 that $\sigma = 0$ indicates the limit of no friction in x-direction on the wall. Thus, a plug like velocity in the channel will appear and the flow tends to diverge.[18,22] It is also noted that the slip velocity for bb boundary condition is not zero for micro flows in the lattice Boltzmann model at $\sigma = 1$. We consider that the bb condition does not give a stick boundary in the model of micro gas because the slip velocity actually depends on τ but τ is not equal to zero for a real gas. Comparing with the Hsieh's[39] results, we find that the numerical result is the best at $\sigma = 0.7$ under

the smooth boundary condition, which is the same as the result of Tang *et al.*[26] As the roughness increases, compared with Cao's[10] results, the accommodation coefficient becomes $\sigma \to 1$. This is also supported by the experiment of Sazhin *et al*[40] in which $\sigma = 0.71$ for the surface of clean silver and $\sigma = 0.935$ for the surface of glass work for Helium gas. Generally, the accommodation coefficient σ depends on the geometry of the solid wall and the species of the gas. As mentioned above the value of the accommodation coefficient is $\sigma \in (0.7, 1)$ when the relative roughness is $\Delta \in [0, 0.078]$, it is approximately taken as $\sigma = 0.9$ in our simulations for the convenient comparability.

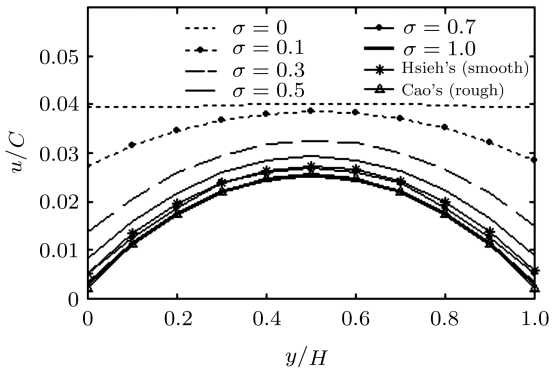


Fig.3. The effect of σ on slip velocity at $x = L/2$ and $Kn = 0.055$.

3. Effects of surface roughness

3.1. Gas parameters and computational condition

There are two methods to handle the inlet and the outlet of the channel in the lattice Boltzmann model for micro Poiseuille flows, i.e. the velocity driven flow and the pressure driven flow.[41] We assume that micro flows are driven by a constant pressure gradient, and the difference of pressure is given by the pressure of the inlet and the outlet of the channel. The pressure boundary condition introduced by Zou and He[41] is applied to handle the inlet and the outlet of the microchannel. From the continuity equation, it is clear that u increases steadily. Thus the density constantly drops along x-direction and the Knudsen numbers of the inlet and the outlet are different. The Knudsen number at the outlet of the microchannel is employed for the consistent expression.

The outlet pressure is taken as a standard atmosphere, the pressure ratio of the inlet to the outlet is $P_{\rm in}/P_{\rm out} = 2$. Nitrogen and helium will be investigated, which are two familiar noble gases in MEMS and represent a larger molecule gas and a smaller molecule gas respectively. Their physical parameters of the two gases are listed in Table 1.

Table 1. The physical parameters of nitrogen and helium.

gas	T/K	R/(J/kg·K)	$\mu_{\rm out}$/(kg/m·s)	$\rho_{\rm out}$/(kg/m^3)	λ/m
nitrogen	314	296.8	1.75×10^{-5}	1.0883	0.066×10^{-6}
helium	314	2076.9	1.92×10^{-5}	0.1553	0.192×10^{-6}

3.2. The influence of fractal levels and grid resolution

The fractal characteristic makes the simulation complicated over other models of regular boundary obstacles. To investigate the influences of the fractal levels and grid resolution on the numerical results, we design a microchannel with $H = 1.2\,\mu$m, $L = 5\,H$ and $\Delta = 0.048$ to investigate influence of the fractal levels and grid resolution on the simulation. The dimension of the fractal boundary curve is about $D \approx 1.2$, which agrees with the experimentally measured roughness in Ref.[42]. The space step of the model is taken as 60nm, 40nm, 30nm and 24nm so that the resolution of the system is $Nx \times Ny = 101 \times 21$, 151×41, 201×41 and 251×51, respectively. Figure 4(a) shows the fractal levels in different system sizes and Fig.4(b) shows the maximum velocity $U_{\rm m}$ at $x = L/2$ in the microchannel. We find that $U_{\rm m}$ does not converge to a fixed value but decreases gradually as the used grid resolution increases. This reason can be explained by the energy dissipation in the more and more tips of the fractal curve as the grid resolution increases. Comparing with a square wave type boundary, we find that the relative errors of the four above grid resolutions are all less than 5% in the aforementioned computational conditions. The best-matching grid resolution of 201×41 will be used in the following simulations to study the roughness effects on the mass flow rate and the resistance coefficient.

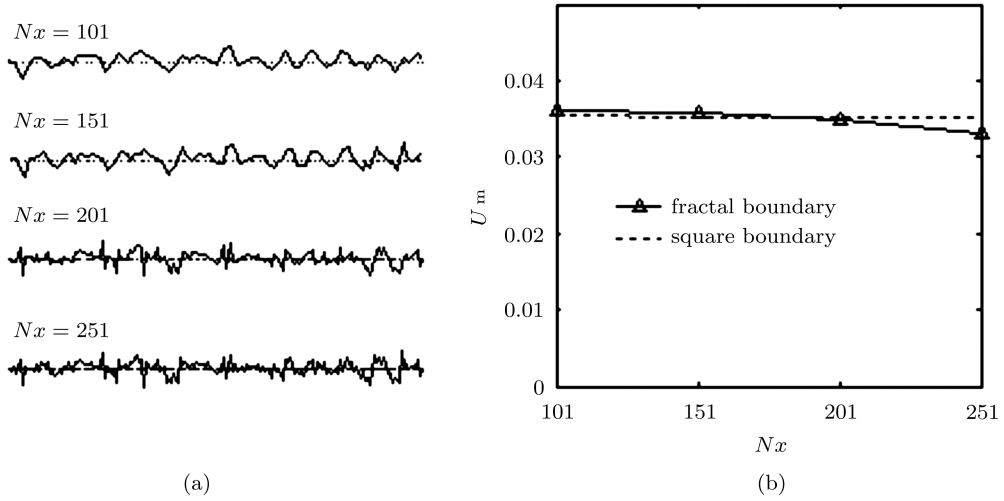


Fig.4. (a) The fractal levels and grid resolution. (b) The effect of the grid resolution on velocity at $x = L/2$.

3.3. Roughness effect on the velocity field

Figure 5 magnifies the velocity field in a self-affine fractal. It is shown that the velocity vectors turn around and the streamlines is distorted in the vicinity of the rough wall. It means that there is additional momentum loss near the wall. There exists significant deviation from the conventional theory in the previous experimental data of water flows.[5,6] The surface roughness may be one of the main attributed factors. Mala and Li[5] introduces a roughness viscosity of liquid to account for this additional momentum transfer, namely the viscosity near the rough wall is no longer taken as a constant. This interpretation is also applicable for gas flows.

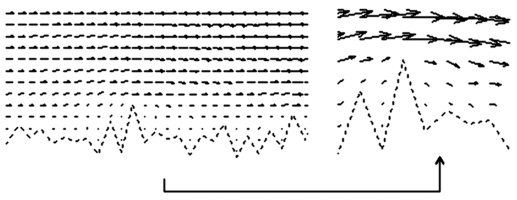


Fig.5. The velocity field in rough boundary with a self-affine fractal surface of $\Delta = 0.048$.

3.4. Roughness effect on the mass flow rate

The micro flows are very sensitive to the nature of the boundary interaction but the interaction cannot be directly measured. Thus it is of great importance to study the mass flow rate and the resistance coefficient through the microchannel to analyse the boundary interaction.[43] The relations between the relative mass flow rate and the roughness are plotted in Fig.6, in which relative mass flow rate is defined as $m/\bar{m}$, $\bar{m}$ is the mass flow rate of nitrogen or helium under the smooth boundary condition. In the macro flows, the mass flow rate is independent of the surface roughness when the relative roughness is less than 5% due to the 'hydraulic smooth'.[10] However, the roughness effect in micro flows becomes significant. It is shown in Fig.6 that the relative mass flow rate descends greatly as the relative roughness increases. The relative mass flow rate of nitrogen drops 6.7% at $\Delta = 0.025$ and 24.7% at $\Delta = 0.078$. It can be explained by the fact illuminated in Fig.5 that reverse flow or small eddies appear in the vicinity of the wall and additional energy is dissipated when the roughness is enhanced. Under

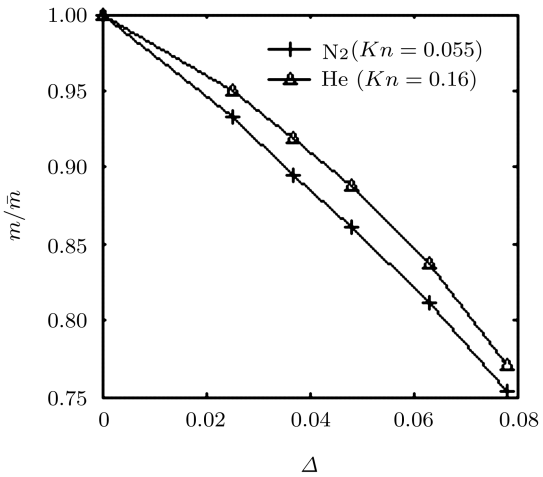


Fig.6. The mass flow rates at various relative roughnesses for nitrogen and helium.

the condition of a same roughness, the ratio of the relative mass flow rate of nitrogen is decreased, the decrease is larger than that of helium. The relative mass flow rate of nitrogen at smaller Knudsen numbers nearly descends linearly, whereas that of helium at higher Knudsen numbers drops rapidly.

3.5. Roughness effect on the resistance coefficient

The relation between the pressure gradient and the velocity of the flow is denoted by the resistance coefficient:[44]

$$C_f = -\frac{\mathrm{d}P}{\mathrm{d}x} \cdot \frac{2H}{\rho u^2}. \tag{18}$$

where P is the pressure and u is the velocity. The relative resistance coefficient C_f/C_{f0} is considered to investigate the deviation of the resistance coefficient from the smooth boundary, where C_{f0} is the resistance coefficient at the outlet of the channel with a smooth boundary. Figure 7 shows the relative resistance coefficient distributions of nitrogen at various roughnesses. The effects of the roughness and the rarefaction on the relative resistance coefficient are strongly coupled in the microchannel, namely the relative resistance coefficient will lessen as the velocity increases due to the compressibility of the gas, whereas the relative resistance coefficient will enhance as the relative roughness increases due to the effect of roughness. The ratio is $C_{f\Delta=0.048}/C_{f\Delta=0} = 2.8$ in Cao's[10] molecular dynamic simulation in which the boundary is described by random triangular wave, and the other parameters are $H = 0.1\mu$m, $A = 4.8$nm (namely the relative roughness $\Delta = 0.048$) and $Kn = 0.055$. The ratio is $C_{f\Delta=0.05}/C_{f\Delta=0.01} = 2.1$ in Rawool's.[45] three-dimensional simulation, in which the surface roughness is described by rectangular and triangular obstructions spaced $200 - 300\mu$m, and the system size is $100\mu\text{m} \times 100\mu\text{m} \times 1000\mu\text{m}$, $Re = 40$. The result of $C_{f\Delta=0.048}/C_{f\Delta=0} = 1.6$ as shown in Fig.7 is consistent with the simulations of Cao and Rawool.

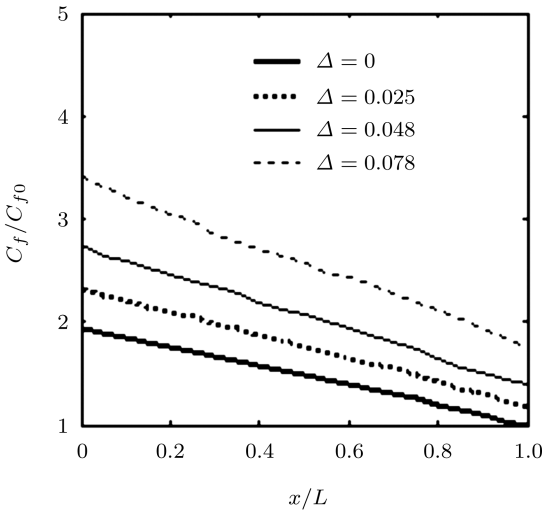


Fig.7. The relative resistance coefficient distributions of nitrogen ($Kn = 0.055$).

4. Conclusions

The roughness effect combining with effects of rarefaction and compressibility is studied by a lattice Boltzmann model at high Knudsen numbers for the two-dimensional microchannel gas flows of nitrogen and helium. To realize this task, a self-affine fractal boundary microchannel is modelled and then the relaxation time and the tangential momentum accommodation coefficient are discussed. By this model, we study and analyse the effects of surface roughness on the velocity field, the mass flow rate and the friction coefficient. The relative mass flow rate descends rapidly as the Knudsen number increases. It can be explained by the fact that reverse flows or small eddies appear in the vicinity of the wall and additional energy is dissipated when the roughness is enhanced. The effects of the roughness and the rarefaction on the relative resistance coefficient are strongly coupled, namely the resistance coefficient lessens as the velocity increases due to the compressibility of the gas, whereas resistance coefficient enhances as the roughness increases. These phenomena differing from macroscopic flows are of great importance in understanding the characteristics of the rarefied gas flows.

References

[1] Moody L F 1944 *ASME Trans* **66** 671

[2] Taylor J B, Carrano A L and Kandlikar S G 2006 *International Journal of Thermal Sciences* **45** 962

[3] Gad-el-Hak M 2003 *International Journal of Heat and Mass Transfer* **46** 3941

[4] Turner S E, Lam L C, Faghri M and Gregory O J 2004 *Journal of Heat Transfer-Transactions of the ASME* **126** 753

[5] Mala G M and Li D Q 1999 *International Journal of Heat*

and Fluid Flow **20** 142
[6] Shen S, Xu J L, Zhou J J and Chen Y 2006 *Energ. Convers. Manage.* **47** 1311
[7] Sugiyama W, Sawada T and Nakamori K 1996 *Vacuum* **47** 791
[8] Sun H W and Faghri M 2003 *Numerical Heat Transfer Part a-Applications* **43** 1
[9] Ding Y T, Yao Z H and Shen M Y 2002 *Chin. Phys.* **11** 869
[10] Cao B Y, Chen M and Guo Z Y 2006 *International Journal of Engineering Science* **44** 927
[11] Cao B Y, Chen M and Guo Z Y 2004 *Chin. Phys. Lett.* **21** 1777
[12] Cao B Y, Chen M and Goo Z Y 2006 *Acta Phys. Sin.* **55** 5305
[13] Nie X B, Doolen G D and Chen S Y 2002 *J. Stat. Phys.* **107** 279
[14] Lim C Y, Shu C, Niu X D and Chew Y T 2002 *Phys. Fluids* **14** 2299
[15] Shen C, Tian D B, Xie C and Fan J 2004 *Microscale Therm. Eng.* **8** 423
[16] Succi S 2002 *Phys. Rev. Lett.* **89** 064502
[17] Succi S, Smith G and Kaxiras E 2002 *J. Stat. Phys.* **107** 343
[18] Sbragaglia M and Succi S 2005 *Phys. Fluids* **17** 093602
[19] Sbragaglia M and Succi S 2006 *Europhysics Letters* **73** 370
[20] Ansumali S and Karlin I V 2005 *Phys. Rev. Lett.* **95** 260605
[21] Ansumali S, Karlin I V, Frouzakis C E and Boulouchos K B 2006 *Physica A—Statistical Mechanics and Its Applications* **359** 289
[22] Zhang Y H, Qin R S, Sun Y H, Barber R W and Emerson D R 2005 *J. Stat. Phys.* **121** 257
[23] Niu X D, Shu C and Chew Y T 2004 *Europhysics Letters* **67** 600
[24] Shu C, Niu X D and Chew Y T 2005 *J. Stat. Phys.* **121** 239
[25] Guo Z L, Zhao T S and Shi Y 2006 *Phys. Fluids* **18** 067107
[26] Tang G H, Tao W Q and He Y L 2004 *Int. J. Mod. Phys.* C **15** 335
[27] Feng S D, Michihisa T and Ji Z Z 2001 *Chin. Phys.* **10** 587
[28] Bhatnagar P L, Gross E P and Krook M 1954 *Phys. Rev.* **94** 511
[29] Qian Y H, Dhumieres D and Lallemand P 1992 *Europhysics Letters* **17** 479
[30] Guo Z L, Zhao T S and Shi Y 2006 *J. Appl. Phys.* **99** 2185839
[31] Guo Z L, Shi B C, Zhao T S and Zheng C G 2007 *Phys. Rev.* E **76** 056704
[32] Kim S H, Pitsch H and Boyd I D 2008 *Phys. Rev.* E **77** 026704
[33] Tang G H, Tao W Q and He Y L 2005 *Physi. Fluids* **17** 058101
[34] Zhang Y H, Qin R S and Emerson D R 2005 *Phys. Rev.* E **71** 047702
[35] Chen S Y, Martinez D and Mei R W 1996 *Phys. Fluids* **8** 2527
[36] Maxwell J C 1879 *Philosophical Transactions of the Royal Society* **170** 231
[37] Hadjiconstantinou N G 2003 *Phys. Fluids* **15** 2352
[38] Voss R 1988 *Fractals in nature.* In: Peitgen H and Saupe H ed. *The Science of Fractal Images* (Berlin: Springer) p21-69
[39] Hsieh S S, Tsai H H, Lin C Y, Huang C F and Chien C M 2004 *International Journal of Heat and Mass Transfer* **47** 3877
[40] Sazhin O V, Borisov S F and Sharipov F 2001 *Journal of Vacuum Science & Technology a-Vacuum Surfaces and Films* **19** 2499
[41] Zou Q S and He X Y 1997 *Phys. Fluids* **9** 1591
[42] Chen Y P and Cheng P 2003 *International Communications in Heat and Mass Transfer* **30** 1
[43] Sharipov F and Seleznev V 1998 *J. Phys. Chem. Ref. Data* **27** 657
[44] Jang J and Wereley S T 2004 *Microfluid. Nanofluid.* **1** 41
[45] Rawool A S, Mitra S K and Kandlikar S G 2006 *Microfluid. Nanofluid.* **2** 215